JUSTIFICATION OF SCHEME AND PARAMETERS OF PNEUMATIC WORKING BODY FOR PRECISE APPLICATION OF TECHNOLOGICAL MATERIALS IN CROP PRODUCTION

Martin Aller[1], Yevhen Ihnatiev[1, 2], Tormi Lillerand[1], Juri Olt[1]
[1]Estonian University of Life Sciences, Estonia;
[2]Dmytro Motornyi Tavria State Agrotechnological University, Ukraine
martin.aller@emu.ee, yevhen.ihnatiev@emu.ee, tormi.lillerand@emu.ee, jyri.olt@emu.ee

Abstract. At the current stage of development of precision agriculture, there is an important task of creating and justifying energy-efficient working bodies capable of implementing the main ideas and tasks of Agriculture 5.0. This article presents a bench-based investigation of transient pneumatic transport of a discrete portion of granular mineral fertilizer from an autonomous field robot for plant-by-plant application. The experimental matrix included four tube inner diameters (10, 12, 16 and 20 mm), six air pressures (400-900 kPa) and 10 replications for each combination, giving 240 tests. Two synchronized chronographs recorded particle velocity at the inlet and outlet of a 1.0 m tube inclined at 45 degrees. The outlet velocity increased from 16.78-22.64 $m \cdot s^{-1}$ at 400 kPa to 23.14-30.07 $m \cdot s^{-1}$ at 900 kPa, while the transport retention ratio increased from 75.0-87.2% to 77.4-88.8% depending on the tube diameter. The most stable and practically suitable regime for the tested fertilizer was 800-900 kPa with 16-20 mm tubes, where the system combined high outlet velocity, lower relative speed losses and satisfactory repeatability (CV = 1.59-2.15%). The results justify the constructive and technological parameters of prototype pneumatic working unit under controlled bench conditions; field agronomic performance, long-term reliability and fertilizer-formulation effects are identified as future research tasks.

Keywords: agricultural robot, precision agriculture, pneumatic transport, mineral fertilizers.

Introduction

Precision fertilisation has become a key requirement of sustainable crop production because nutrient inputs must be matched to plant demand while limiting losses, labour costs and treatment of non-productive zones [1-3]. Recent reviews show that modern fertiliser systems increasingly combine variable-rate control, sensing, machine vision and robotic execution, particularly in row crops where plant-specific application is technically feasible and agronomically justified [4-7].

Within solid input delivery systems, pneumatic applicators are attractive because compressed air can convey granular material rapidly through closed pipelines, centralise metering, and place fertiliser at several outlets or directly near the target plant [4-6]. At the same time, recent literature identifies unstable discharge, particle retention, pressure losses, row-to-row maldistribution and the limited availability of reliable real-time mass-flow sensing as the bottlenecks of pneumatic fertilization [8; 9].

Recent CFD-DEM and bench studies also show that feeder geometry, spiral conveying paths and particle-material interaction parameters can markedly affect discharge stability, tube accumulation and branch-to-branch uniformity in pneumatic fertilizer systems [21, 22]. Therefore, for robotic plant-level application the remaining engineering gap is not only dose metering, but also fast and repeatable transient transport of a single metered portion through a short applicator tube.

Modern applicators are also becoming more intelligent at the control level. A self-calibration variable-rate fertilisation system reduced the steady-state error of fertiliser-shaft speed to 0.13 $r \cdot min^{-1}$ and improved distribution stability across vehicle speeds, while an AI-enabled site-specific applicator placed fertiliser near detected plants at the recommended dosage [10]. Recent horticultural reviews therefore identify machine vision, multimodal sensing and implement interoperability as decisive for plant-specific fertilisation in perennial crops [6; 7].

This tendency is especially relevant for blueberry plantations, where fertilising the spaces between bushes is economically inefficient and environmentally undesirable. In a recent study on low-bush blueberry fertilisation, a screw-based dispenser designed for Yara Mila Cropcare NPKS-8-11-23-29 achieved the desired 20 g target range in 90% of cases, showing that discrete dose formation can already be performed with acceptable accuracy [11] and in combination with an unconventional static flight screw solution could possibly provide increased throughput efficiency [12].

Accurate metering alone does not guarantee accurate placement, because the discrete dose must be transported through the applicator tube within a predictable time window. Lillerand et al. proposed a

two-stage pneumatic device for an agro-robot, in which a single fertiliser portion is accumulated in a chamber and then ejected through an inclined tube by compressed air; preliminary validation reported a relative error of about 3% for a 0.01 kg portion and about 9.5% for a 0.04 kg portion [13].

The aim of the article is to propose the schematic design and operating parameters of a pneumatic working unit for precise application of technological materials by validating mathematical model with experimental measurements obtained from a test bench and determining optimal operating regimes.

Materials and methods

This study combines theoretical modelling with experimental validation of a pneumatic working unit for precision fertilization. In the first stage, the motion of a metered portion inside the applicator tube is described mathematically. In the second stage, the model is verified against measurements obtained on a laboratory test bench. The general approach follows the previously reported theoretical treatment of a pneumatic precision fertilization device, in which a discrete portion is accelerated and transported through the applicator tube by compressed air [13]. Under these conditions, the most important output variables are the portion transit time and its exit velocity. In practical site-specific application, the transport process must also be synchronized with the control signal and the spatial coordinates of the target point so that the metered portion reaches the root zone at the correct moment [7]. From the engineering point of view, this means that the pneumatic unit cannot be evaluated only as a flow device; it must also be considered as a time-sensitive delivery system [13].

A simplified description of the process may be written by considering the transported portion as a body subjected to the driving force generated by the air stream and the opposing effects of gravity, friction, and local resistances. In a general form, the equation of motion may be expressed as:

$$m\frac{dv}{dt} = F_{air} - F_f - F_{res} - mg\sin\alpha \,, \tag{1}$$

where m – mass of the metered portion, kg;
v – instantaneous particle velocity, $m \cdot s^{-1}$;
F_{air} – pneumatic driving force, N;
F_{fr} – friction force, N;
F_{res} – local-resistance and particle-wall interaction force, N;
g – gravitational acceleration, $m \cdot s^{-2}$;
α – tube inclination angle, deg.

Equivalent particle diameter D was calculated as the geometric mean of the particle length, width and thickness. This parameter was used to represent the size of irregular granules by a single characteristic dimension for further analysis of pneumatic transport behaviour [14].

$$D = \sqrt[3]{LWT} \,, \tag{2}$$

where L, W, T – particle length, width and thickness accordingly, mm.

Sphericity was calculated as the ratio of equivalent particle diameter to particle length. It was used to describe the particle shape by indicating how closely the granule approached a spherical form [13; 14].

$$\varphi = \frac{D}{L} \,, \tag{3}$$

where φ – sphericity.

The experimental material was a commercial granular complex fertilizer, YaraMila Cropcare NPK(S) 8-11-23(29), with nominal nutrient composition N-P_2O_5-K_2O-SO_3 = 8-11-23-29. The metered portion was treated as a discrete dose of one fertilizer batch; consequently, particle size and sphericity were controlled material properties rather than independent experimental factors. The 2-4 mm size fraction prevailing in this type of product is important for pneumatic transport, because it affects drag, wall collisions and the probability of temporary retention. The influence of fertilizer morphology is therefore discussed separately and proposed as a variable for future multi-material tests.

The timing sequence used in the pneumatic transport experiments is shown in Fig. 1. It shows the relation between the valve control signal, the air pulse, and the moments when the fertilizer portion passes the first and second chronographs, which makes it possible to determine the transport time, average conveying velocity, and the total response time of the system. The experimental material and the laboratory equipment used in the pneumatic transport study are presented in Fig. 2. Test dosages were weighed using a Kern ABJ 220-4NM scale. The figure provides an overview of the sample preparation procedure and the test bench used for evaluating the movement of a metered granular portion under controlled pneumatic conveying conditions.

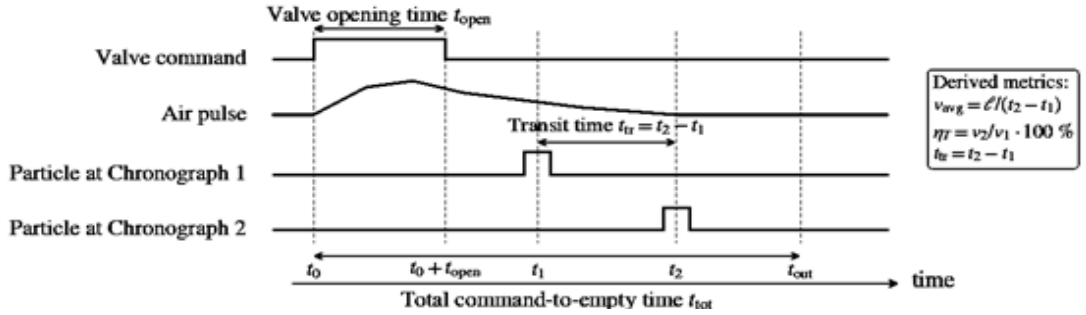

Fig. 1. **Timing logic from command impulse to outlet**

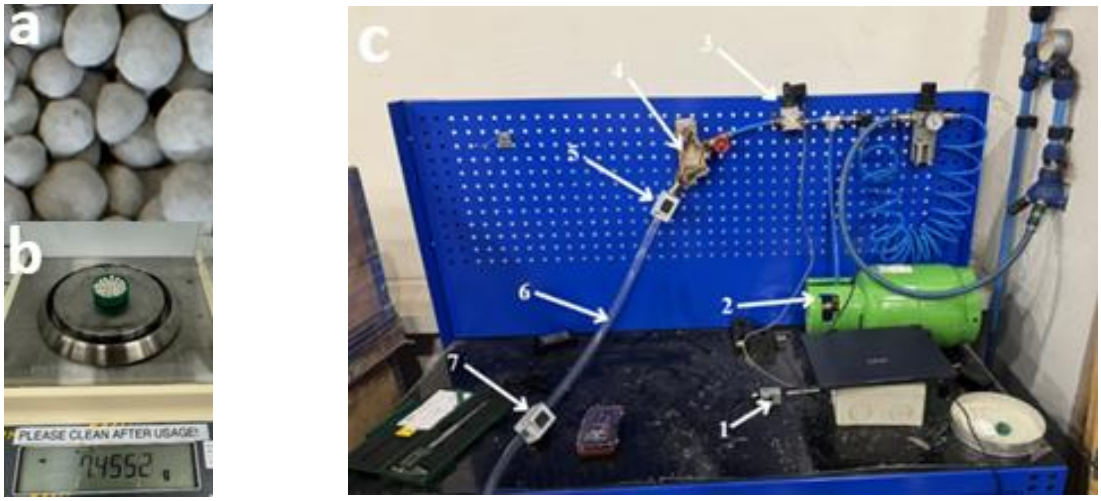

Fig. 2. **Equipment used for testing:** a – fertilizer; b – dosage for testing; c – test bench; 1 – valve control system; 2 – compressed air source; 3 – solenoid valve; 4 – collecting chamber; 5 – chronograph 1; 6 – applicator tube; 7 – chronograph 2

Table 1 summarizes the experimental factors, measured signals and derived response variables used in the study. From the measured timestamps, the transit time was calculated as $t_{tr} = t_2 - t_1$, the average transport velocity as $v_{avg} = l / t_{tr}$, the speed loss as $\Delta v = v_1 - v_2$, the transport retention as $\eta_t = (v_2 / v_1) \cdot 100\%$, and the repeatability as $CV = (S / \bar{x}) \cdot 100\%$. Where t_1 and t_2 are the inlet and outlet timestamps, l is the measurement-section length, v_1 and v_2 are particle speeds at the two chronographs, S is the standard deviation, and $\bar{x}$ is the mean value.

The compressed-air line was operated with a pressure regulator in the 400-900 kPa range, and the pressure setting was checked directly before each test series. The same normally closed solenoid valve, control unit and compressed-air source were used in all experiments; therefore, their response delay was constant within the factorial comparison. Applicator tubes were smooth transparent polymer tubes with the inner diameters listed in Table 1, the same length $l = 1.0$ m and the same inclination angle $\alpha = 45$ deg. The chronographs were synchronized to the valve-control signal and checked before the test series to maintain a common time base. All tests were conducted under stable indoor laboratory conditions; temperature and relative humidity were not deliberately varied.

For each pressure-diameter combination, the test sequence consisted of pressure stabilization, dose placement in the collecting chamber, valve activation, registration by chronograph 1 and chronograph

2, and complete emptying of the tube before the next repetition. Each combination was repeated 10 times. The statistical processing included the mean value, standard deviation, coefficient of variation, speed loss, transport retention ratio and pressure sensitivity. The pressure effect was additionally summarized by least-squares linear regression of outlet velocity versus pressure for each tube diameter. Because the objective is engineering parameter justification, the statistical interpretation is limited to bench repeatability and trend consistency rather than field-scale inference.

Table 1

Proposed experimental-factor and response matrix for the pneumatic transport study

Group	Symbol	Description	Role in model or experiment
Material	–	Granular fertilizer in the current bench dataset	Blocking factor for particle-property effects
Pressure	p, kPa	400, 500, 600, 700, 800, 900	Main driving factor
Tube inner diameter	d, mm	10, 12, 16, 20	Controls pressure loss and particle-cloud confinement
Geometry	l, α	l = 1.0 m; α = 45°	Transport distance and gravity effect
Signals	t_1, t_2, $p(t)$, T	Common time base for time stamps, pressure and temperature	Used to derive t_{tr} and v_{avg}
Derived responses	v_1, v_2, Δv, η_t, CV	Calculated parameters	Used for performance comparison
Replications	n	10 tests for each tube and pressure. A total of 240 tests	Ensures repeatability assessment

Results

The tests showed a clear and mechanically consistent effect of both operating pressure and applicator tube diameter on the response of the pneumatic working unit. To address the complete-factor processing, the full mean response matrix for all pressures and diameters is reported in Table 2.

Table 2

Results of experimental studies and statistical parameters

Pressure p, kPa:	**Tube inner diameter d, mm**							
	10		**12**		**16**		**20**	
	v_1, m·s^{-1}	**v_2, m·s^{-1}**	**v_1, m·s^{-1}**	**v_2, m·s^{-1}**	**v_1, m·s^{-1}**	**v_2, m·s^{-1}**	**v_1, m·s^{-1}**	**v_2, m·s^{-1}**
400	22.38	16.78	23.89	18.76	25.62	21.18	25.97	22.64
500	23.88	18.05	25.41	20.11	27.08	22.57	27.55	24.13
600	25.39	19.32	26.92	21.45	28.53	23.96	29.13	25.61
700	26.89	20.60	28.44	22.80	29.99	25.35	30.71	27.10
800	28.40	21.87	29.95	24.14	31.44	26.74	32.29	28.58
900	29.90	23.14	31.47	25.49	32.90	28.13	33.87	30.07
kv_2, m·s^{-1} per 100 kPa	1.26		1.34		1.43		1.45	
Mean η_t, %	76.0		79.9		84.5		87.4	

The values correspond to the processed mean chronograph data used to prepare Figs. 3-6; retention is calculated as $\eta_t = v_2 / v_1 \cdot 100\%$. The numerical results given in Table 2 support this interpretation by condensing the low- and high-pressure behaviour and linking the high-pressure regime to its practical engineering assessment [8; 9; 15].

As shown in Figs. 3 and 4, the chronograph readings increased with pressure at both positions, while the tube diameter influenced the magnitude and stability of the response. The largest outlet values were obtained with the 16 and 20 mm tubes at the higher-pressure, indicating more favourable conditions in this operating range. Figs. 5 and 6 further evaluate the same results in terms of transport loss and retention behaviour, which allows the outlet performance to be interpreted more quantitatively [9; 15].

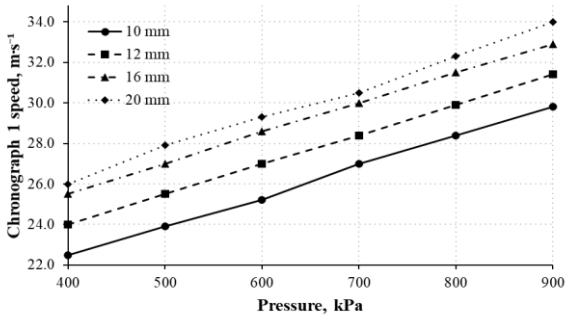

Fig. 3. **Particle speeds from chronograph one**

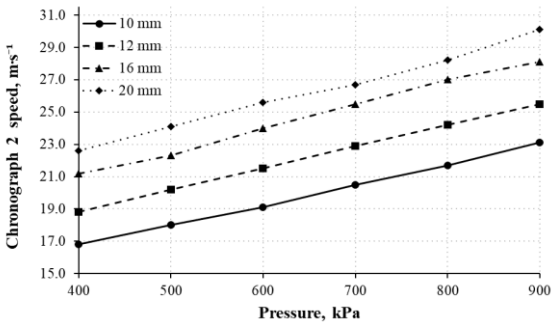

Fig. 4. **Particle speeds from chronograph two**

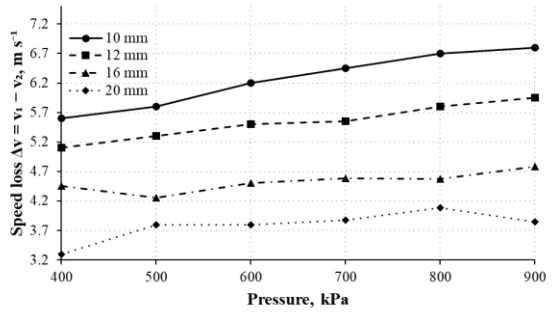

Fig. 5. **Speed difference between the inlet and outlet**

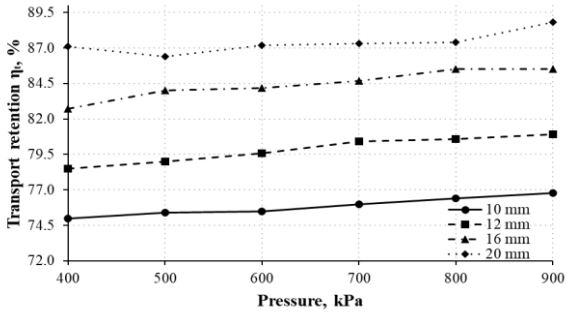

Fig. 6. **Transport retention ratio**

The mean effect of the tube diameter at both measuring positions is illustrated in Fig. 7, whereas Fig. 8 shows the outlet-response operating map and identifies the most suitable working region. The 10 mm tube was consistently the least favourable option, while the 12 mm tube improved the response but still exhibited a larger drop between inlet and outlet than the two wider configurations. The repeatability of the measurements was generally satisfactory. For the first chronograph, the average coefficient of variation remained between 1.24 and 1.86% depending on the tube diameter, while for the second chronograph the corresponding range was about 1.59 to 2.15%. Similar sensitivity to the interaction between transport geometry and actuation control has been reported for portable variable-rate applicators developed for perennial crops [16].

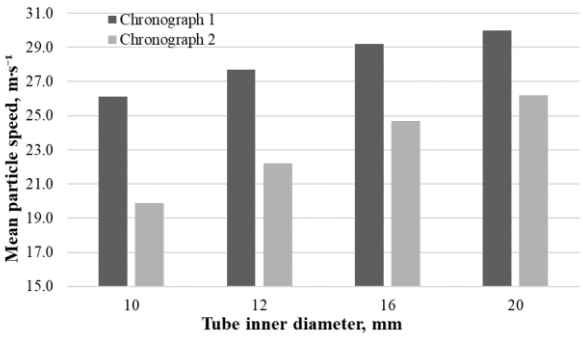

Fig. 7. **Mean particle speeds by tube inner diameters**

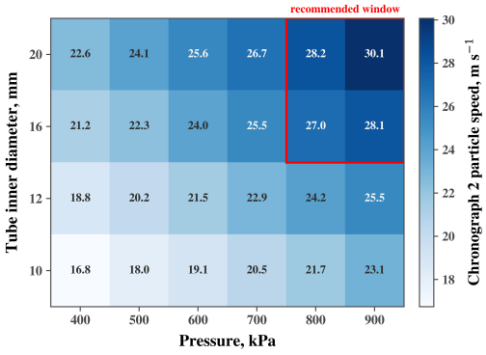

Fig. 8. **Operating map for selecting optimal parameters**

From a systems perspective, temporal repeatability of this kind is important because automated experimental platforms and field validation environments require consistent synchronisation between control signal, vehicle motion, and material release [17]. The present results primarily justify the pneumatic scheme and range of operating parameters rather than proving agronomic benefit directly.

Nevertheless, transport behaviour must ultimately be considered together with fertiliser formulation, because eco-friendly and controlled-release fertilisers can change the optimal balance

between fast delivery, local placement, and post-placement nutrient release [18; 19]. Biochar-based formulations further underline that delivery hardware and fertiliser chemistry have to be co-designed when the goal is to reduce nutrient losses while maintaining local application accuracy [20].

Comparison with the theoretical description confirms the expected signs of the main terms in Eq. (1). Raising the air pressure increases the pneumatic driving force, and the measured outlet speed increased by 32.8-37.9% when the pressure was raised from 400 to 900 kPa, depending on the tube diameter. Increasing the tube diameter reduced the relative role of wall contacts and local losses: at 400 kPa the retention ratio grew from 75.0% for d = 10 mm to 87.2% for d = 20 mm, and at 900 kPa from 77.4% to 88.8%. Thus, the simplified model is adequate for selecting the operating region, although it is not a particle-resolved CFD-DEM model for predicting every collision or rebound event.

Particle size and sphericity affect the results through aerodynamic drag, rolling and sliding friction, collision angle, wall rebound and the probability of arching or temporary retention. Less spherical granules have less repeatable contact geometry and can show stronger interaction with the tube wall; larger granules require higher drag force for acceleration, whereas fine fractions may increase segregation and dust-related losses. Because one commercial fertilizer batch was used, these properties were fixed rather than varied independently. Future tests should therefore separate the batch into sieve fractions and compare at least two fertilizer products with different sphericity and coating strength. This is especially important for controlled-release, organic and brittle granules, because recent studies connect particle phenotype, mechanical strength and interaction parameters with handling, transport and application quality [23-26].

Compared with continuous pneumatic centralized fertilizer-discharge systems, the present study focuses on the transient delivery of a single dose through a short robotic applicator. Consequently, the outlet-speed coefficient of variation (about 1.59-2.15%) should not be interpreted as the same quality indicator as branch mass-distribution CV. Nevertheless, the observed timing repeatability is compatible with the engineering aim of synchronizing valve opening with robot motion. Recent CFD-DEM and bench or field studies report branch or field CV values of about 3.96-5.27% after structural optimization, confirming that suitable tube geometry and controlled airflow can considerably improve pneumatic fertilizer distribution [21; 22]. The proposed 16-20 mm and 800-900 kPa operating region is therefore consistent with the broader trend toward larger effective flow passages and stable air-fertilizer mixing, while still requiring validation under robot vibration, field humidity and different fertilizer formulations.

Conclusions

1. The tests showed that the proposed pneumatic working unit can reliably transport and deliver granular technological material under controlled bench conditions.
2. Air pressure and applicator tube diameter had the strongest effect on transport performance. Higher pressure increased particle velocity, while larger tube diameters improved outlet conditions and reduced transport losses.
3. For the tested fertilizer and bench setup, the most suitable operating range was 800-900 kPa with 16-20 mm applicator tubes, where the system gave the best overall outlet response.
4. The experimental trends agreed with the theoretical description: higher pressure increased the pneumatic driving term, while larger tube diameters reduced relative outlet losses. The model is therefore suitable for engineering parameter selection, but detailed particle-resolved prediction requires additional CFD-DEM or multi-material calibration.
5. The conclusions are limited to the laboratory bench and one fertilizer batch. Field synchronization, agronomic response, long-term clogging or abrasion, and the effect of different particle-size and sphericity classes should be addressed in further research.

Author contributions

M.A.: conceptualization, bench experiments, data analysis, and writing original draft preparation. Y.I.: methodology, mathematical modelling, and writing-review and editing. T.L.: supervision, interpretation of results, and writing-review and editing. J.O.: funding and editing.

References

[1] You L., Ros G.H., Chen Y., Zhang F., de Vries W. Optimized agricultural management reduces global cropland nitrogen losses to air and water. Nature Food, vol. 5, no. 12, 2024, pp. 995-1004.
[2] Lam S.K., Wille U., Hu H.-W., Caruso F., Mumford K., Liang X., Pan B., Malcolm B., Roessner U., Suter H., Stevens G., Walker C., Tang C., He J.-Z., Chen D. Next-generation enhanced-efficiency fertilizers for sustained food security. Nature Food, vol. 3, no. 8, 2022, pp. 575-580.
[3] Maaz T.M., Sapkota T.B., Eagle A.J., Kantar M.B., Bruulsema T.W., Majumdar K. Meta-analysis of yield and nitrous oxide outcomes for nitrogen management in agriculture. Global Change Biology, vol. 27, no. 11, 2021, pp. 2343-2360.
[4] Huck C., Gobrecht A., Salou T., Bellon-Maurel V., Loiseau E. Environmental assessment of digitalisation in agriculture: A systematic review. Journal of Cleaner Production, vol. 472, 2024, article 143369. DOI: 10.1016/j.jclepro.2024.143369
[5] Dey B., Ahmed R. A comprehensive review of AI-driven plant stress monitoring and embedded sensor technology: Agriculture 5.0. Journal of Industrial Information Integration, vol. 47, 2025, article 100931. DOI: 10.1016/j.jii.2025.100931
[6] Upadhyay A., Chandel N.S., Singh K.P., Chakraborty S.K., Nandede B.M., Kumar M., Subeesh A., Upendar K., Salem A., Elbeltagi A. Deep learning and computer vision in plant disease detection: a comprehensive review of techniques, models, and trends in precision agriculture. Artificial Intelligence Review, vol. 58(3), 2025, article 92.
[7] Tsoulias N., Paraforos D.S. Real-time applications in perennial trees and vegetables - a review. Smart Agricultural Technology, vol. 11(4), 2025, article 100918.
[8] Zhang J., Zhuang Q., Liu G., Zhang Z., Pan J., Xiao P. Review of the granular fertilizer mass flow rate measurement techniques for variable-rate fertilization drills. Computers and Electronics in Agriculture, vol. 234, 2025, article 110312.
[9] Zhang L., Yuan W., Jin C., Feng Y., Liu G., Hu Y. Research progress on key mechanical components of the pneumatic centralized fertilizer discharge system. Applied Sciences, vol. 14, no. 9, 2024, article 3884.
[10] Gao Y., Feng K., Yang S., Han X., Wei X., Zhu Q., Chen L. Design and experiment of an unmanned variable-rate fertilization control system with self-calibration of fertilizer discharging shaft speed. Agronomy, vol. 14, no. 10, 2024, article 2336.
[11] Kuennapuu K., Lillerand T. Feasibility of screw dosing system for low-bush blueberry fertilization. Proceedings of the 24th International Scientific Conference “Engineering for Rural Development”, May 21-23, 2025, Jelgava, Latvia, pp. 687-693.
[12] Moelder K., Lillerand T. Design and feasbility analysis of vertical static flight screw conveyor usage in granulated fertilizer transportation. Proceedings of the 24th International Scientific Conference “Engineering for Rural Development”, May 21-23, 2025, Jelgava, Latvia, pp. 423-428. DOI: 10.22616/erdev.2025.24.tf090
[13] Lillerand T., Liivapuu O., Ihnatiev Y., Olt J. Theoretical study of a pneumatic device for precise application of mineral fertilizers by an agro-robot. AgriEngineering, vol. 7, no. 10, 2025, article 320. DOI: 10.3390/agriengineering7100320
[14] Song X., Dai F., Zhang F., Wang D., Liu Y. Calibration of DEM models for fertilizer particles based on numerical simulations and granular experiments. Computers and Electronics in Agriculture, vol. 204, 2023, article 107507.
[15] Wang L., Cong J., Liu Z., Liao Q., Liao Y., Shi Y., Wang X. Design and experimental analysis of the air-assisted fertilizer apparatus’s distributor using DEM-CFD and high-speed photography. Computers and Electronics in Agriculture, vol. 237, 2025, article 110653.
[16] Quintão I.R., Valente D.S.M., Coelho A.L.d.F., Queiroz D.M., Furtado Junior M.R., Villar F.M.d.M., Rodrigues P.H.d.M. Portable machine with embedded system for applying granulated fertilizers at variable rate. Agriculture, vol. 15, no. 4, 2025, article 361.
[17] Hoffmann M., Chen C., Butterbach-Bahl K., Ewert F., Holz M., Kiese R., Augustin J., Dubbert M. Advancing sustainable agricultural transformation through the synergy of automated experimental platforms and living labs. Nature Communications, vol. 16(1), 2025, article 8418. DOI: 10.1038/s41467-025-64450-7
[18] Jafari M., Mardani A., Aghaei M. A comprehensive review on the development of eco-friendly and controlled-release fertilizers. Journal of Cleaner Production, vol. 411, 2023, article 136685.

[19] Vejan P., Khadiran T., Abdullah R., Ahmad N. Controlled release fertilizer: A review on developments, applications and potential in agriculture. Journal of Controlled Release, vol. 339, 2021, pp. 321-334. DOI: 10.1016/j.jconrel.2021.10.003
[20] Sim D.H.H., Tan I.A.W., Lim L.L.P., Hameed B.H. Encapsulated biochar-based sustained release fertilizer for precision agriculture: A review. Journal of Cleaner Production, vol. 303(1), 2021, article 127018. DOI: 10.1016/j.jclepro.2021.127018
[21] Dong W., Zhang X., Jiang Z., Hu X., Ge Y., Zhang L. Study on structure design and parameter optimization of diversion rifled feeder based on CFD-DEM. Agriculture, vol. 15, no. 3, 2025, article 351. DOI: 10.3390/agriculture15030351
[22] Zhang L., Yuan W., Feng Y., Jin C., Liu G., Xie S. Design and experiment of spiral conveying pipe in pneumatic centralized fertilizer discharge system. PLoS ONE, vol. 20, no. 6, 2025, article e0320126. DOI: 10.1371/journal.pone.0320126
[23] Lei X., Wu W., Deng X., Li T., Liu H., Guo J., Li J., Zhu P., Yang K. Determination of material and interaction properties of granular fertilizer particles using DEM simulation and bench testing. Agriculture, vol. 13, no. 9, 2023, article 1704. DOI: 10.3390/agriculture13091704
[24] Xin M., Jiang Z., Song Y., Cui H., Kong A., Chi B., Shan R. Compression strength and critical impact speed of typical fertilizer grains. Agriculture, vol. 13, no. 12, 2023, article 2285. DOI: 10.3390/agriculture13122285
[25] Sun L., Chen X., Chen Z., Jing L., Wang J., Cao X., Fu S., Jiang Y., Zhang H. Crushing force prediction method of controlled-release fertilizer based on particle phenotype. Agriculture, vol. 14, no. 12, 2024, article 2235. DOI: 10.3390/agriculture14122235
[26] Jotautiene E., Bivainis V., Karayel D., Mieldazys R. Theoretical and experimental verification of the physical-mechanical properties of organic bone meal granular fertilizers. Agronomy, vol. 14, no. 6, 2024, article 1171. DOI: 10.3390/agronomy14061171